Improving Carbon Nanotubes Sensor Time Response and Responsivity Using Constant-Power Activation

Mengxing Ouyang, Wen J. Li, *Fellow, IEEE*, Philip H. W. Leong, and Ka Wai Wong

***Abstract*—For classical resistive-based signal transduction methods, constant-power (CP) and constant-current (CC) activation methods have been utilized since the 1970s. However, since the discovery of carbon nanotube (CNT) in 1991, not much has been done in the past 20 years in terms of comparing how these transduction methods affect CNT-based sensor output. In this paper, we compare the responsivity, sensitivity, transient response, and instantaneous power consumption of CNT sensors activated by CC and CP modes. As an application example, multiwall CNTs were functionalized with COOH groups and used as ethanol (alcohol) vapor sensors. A CP control circuit has been built in order to test the CNT-based ethanol vapor sensors. A commercial source meter was used to activate the CNT sensors under CC mode. The CP configuration was shown to be effective in minimizing the self-heating effect, which is a significant factor that affects sensor performance, especially for resistive-based sensors. Compared to CC mode, CP mode of sensor activation demonstrated not only shorter transient response time but also larger responsivity, especially when the input activation power is low or ethanol concentration is relatively high.**

***Index Terms*—Alcohol vapor sensor, carbon nanotube (CNT) sensors, constant-power (CP) activation, constant-current (CC) activation, ethanol vapor detection.**

I. Introduction

WITHIN the last decade, carbon nanotube (CNT) sensors have received considerable attention due to their merits such as high surface-to-volume aspect ratio [1], and small size of the sensing element required for a response [2]. Since CNT electronic property is a strong function of its atomic structure, mechanical deformations or chemical doping can induce significant changes in its conductance, which can be detected by electronic systems [3]. The capability of CNTs to serve as chemical sensing elements has been proved worldwide (see [4]). As an example of sensing application for CNT sensor, over the last decade, many research groups have been focusing on the gas adsorption mechanism of CNTs [5]–[8] as well as utilizing CNT-based sensors to detect gases, such as CO_2 [9], NO_2 [10], and ammonia gas [11], etc., CNT gas sensors offer significant advantages over conventional electrical sensors in terms of sensitivity and operating at a significantly lower temperature than conventional metal–oxide-based sensors [12].

A. Activation of CNT Sensors

According to the different structures and properties of the CNT, several sensor activation methods have been adopted in applications, which include *resistive*, *capacitive* and *semiconductive*.

Many of the resistive CNT gas sensors are based on randomly aligned CNT films: some researchers grow CNTs on the substrate [13], while others use CNT/polymer composite [14] as sensing elements. Besides, the method of drop-casting aqueous solutions containing CNTs onto the substrate [15] has also been used. For these resistive sensors, the change in the resistance of the CNT device is utilized as the sensing principle. Our lab has been investigating various resistive CNT sensors in the past decade, such as ethanol [16], pressure [17], and flow sensors [18].

CNT also stands out as a novel material for new breeds of capacitors and has attracted many researchers' attention (see [19]–[21]). The "supercapacitors" made by CNTs exhibit giant capacitances in comparison with those of ordinary dielectric-based capacitors [2]. Snow *et al*. [22] constructed a high-performance chemicapacitor by coating single-wall nanotubes (SWNTs) with chemoselective materials, and indicated that the capacitance of SWNTs was highly sensitive to a broad class of chemical vapors. However, capacitive sensors typically require more complex circuitry to acquire sensor signal.

Moreover, SWNT-based transistors have demonstrated their potential to detect gas molecules [23]. Despite their high sensitivity [24], it is generally difficult to separate semiconductive SWNTs from metallic SWNTs and multiwall nanotubes (MWNTs). Therefore, CNT transistors are not only complex and costly in fabrication, but also suffer from the low sensor yield.

B. Sensor Configuration

It is known that resistive-based sensors can be driven in different configurations, such as CC and CP. A CC system uses a

Manuscript received September 28, 2011; revised December 16, 2011 and January 25, 2012; accepted February 5, 2012. Date of publication February 22, 2012; date of current version May 9, 2012. This work was supported by the Hong Kong Research Grants Council under Project 413906 and by the Hong Kong Innovation and Technology Commission under Project ITS/027/06. The review of this paper was arranged by Associate Editor R. Lake.

M. Ouyang is with the Centre for Micro and Nano Systems, The Chinese University of Hong Kong, Shatin, Hong Kong, SAR (e-mail: mxouyang@mae.cuhk.edu.hk).

W. J. Li is with the Department of Mechanical and Biomedical Engineering, City University of Hong Kong, Kowloon, Hong Kong, SAR (e-mail: wenjli@cityu.edu.hk).

P. H. W. Leong is with the School of Electrical and Information Engineering, The University of Sydney, Sydney NSW 2006, Australia (e-mail: philip.leong@sydney.edu.au).

K. W. Wong is with Chengdu Green Energy and Green Manufacturing Technology R&D Center, Sichuan, China, and also with the Nano and Advanced Materials Institute Limited, Kowloon, Hong Kong (e-mail: kwwong@nami.org.hk).

Color versions of one or more of the figures in this paper are available online at http://ieeexplore.ieee.org.

Digital Object Identifier 10.1109/TNANO.2012.2188641

fixed CC supply and has been widely deployed. Since the input current is constant, electric power of the sensor would increase proportionally to the increase of sensor resistance and further lead to a higher operating temperature, which shortens sensor life and increases zero drift [25]. This is even more critical for CNT-based sensors due to the fact that CNT is a kind of thermal sensitive sensing element, and therefore the instability of operating power and the change of ambient temperature could affect the sensor performance and jeopardize the sensor's reliability. However, in the CP configuration, where a circuitry continuously monitors the resistance of the reference and active (sensing) elements and maintains a sensor's activation power at a certain value, sensor performance is stabilized and possibly optimized since it is not affected by the surrounding temperature. In applications, CP circuit is desirable in various fields, especially for thermal-based sensors [26], such as vacuum sensors, ac power meters, flow sensors, and gas detection sensors in order to compensate for sensor drifts caused by ambient temperature drifts [27]. Some commercial gas sensor companies even recommend their customers to use the products under CP configuration to achieve best performance [28]. However, we note here that compared with CC mode, CP operation usually requires more complex circuit, which tends to induce extra noise to the sensing system and raise the overall sensing system cost.

In order to study and compare CNT sensor performance under these two activation configurations, we built a CP measuring system specifically to power CNT sensors as commercially available CP activation typically supplies too much power to a sensing system. The performance of sensor response based on this system is then compared to sensor response based on using a commercially available CC source meter. As an example, CNT sensors used for ethanol vapor detection were tested using these two activation configurations and the results are reported in this paper.

C. Our Previous Work

Our group has been studying CNT-based ethanol vapor sensor since 2004 [29]. In our previous work, CNTs grafted with several kinds of functional groups have been proven to be sensitive toward ethanol molecules, and their potential to serve as ethanol vapor sensor have been demonstrated. The functional groups not only enhance the responsivity of the ethanol vapor sensor, but also enable CNT sensors to achieve better selectivity toward different variables. In addition, we also evaluated different functional groups through both chemical and physical functionalization methods for the optimization of sensor performance.

In this paper, we will focus on presenting the sensor response results for ethanol vapor sensors based on functionalized CNTs (f-CNTs) with COOH group fabricated by chemical oxidation. These sensors were characterized using both CC and CP configurations. We will present the comparison of the sensor responsivity, sensitivity, and time constant under different ethanol concentration and operating power using these two measuring configurations.

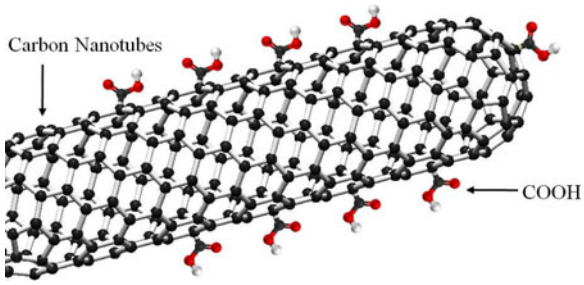

Fig. 1. Chemically f-CNTs with COOH groups.

II. Fabrication of F-CNT-Based Ethanol Sensors

A. Fabrication of f-CNTs

In our experiments, commercially available MWNTs were used for subsequent chemical oxidation and graft of functional group (e.g., –COOH) along the sidewall and the tube ends of the CNTs (see Fig. 1) in our laboratory. The CNTs were first purified, and then sonicated. Finally, after centrifugation, the functionalized MWNTs were collected, washed, and re dispersed in solvent for use. Details of the functionalization process of CNTs are presented in [27].

B. Fabrication of Sensing Elements by Dielectrophoresis (DEP) Manipulation

DEP manipulation was used to form CNT linkage between microelectrodes [30], which were fabricated on the Si substrate by conventional microphotolithographic process. During the sensing element formation process, a droplet of f-CNT solution (solvent) was transferred to the gap between a pair of Au microelectrodes, which were simultaneously excited by an ac bias voltage. After a while, the solvent evaporated, leaving f-CNT connection between the two electrode tips. Typically, the two-probe room temperature resistance of the f-CNT-based sensing element range from several tens of kilo-Ohms to several hundreds of kilo-Ohms, depending on the concentration and volume of the solution droplet.

C. Experimental Setup

For the purpose of electrical connection with the measuring unit, the sensor chip was then fixed and wirebonded to a printed circuit board (PCB), where several small holes were drilled for the outlet of ethanol vapor. And then, a plastic cover was put on top of the sensor chip. During the experiments, the ethanol vapor is generated by directing a well-controlled flow of compressed air into the mixed ethanol solution. For CC configuration, a commercial source meter (Keithley 2400 Source Meter) was employed to measure and collect the electrical signals of f-CNT sensors. The experimental setup is illustrated in Fig. 2.

III. Characterization of F-CNT-Based Sensors

A. I–V Characteristics

The *I–V* characteristic of a typical f-CNT-based sensor is shown in Fig. 3. Compared to Ohm's law expectation,

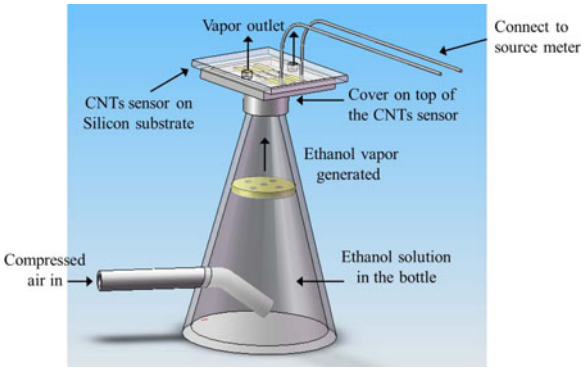

Fig. 2. Experimental setup under constant current mode.

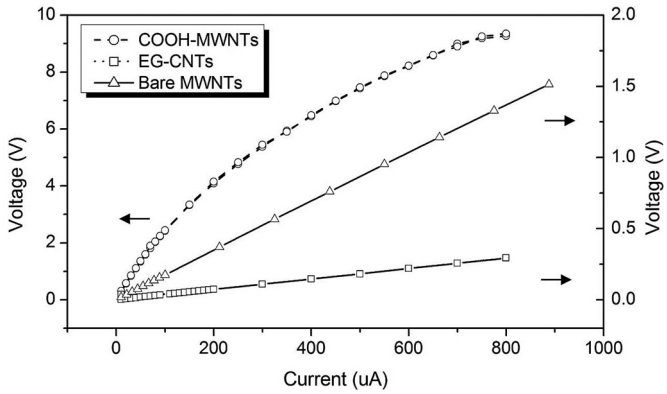

Fig. 3. *I–V* characteristic of different types of CNTs.

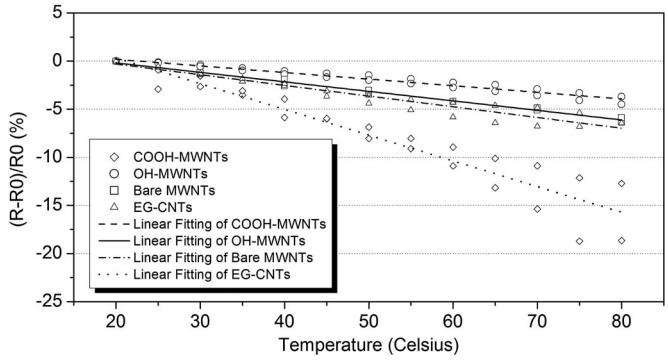

Fig. 4. TCR of different types of CNTs sensors.

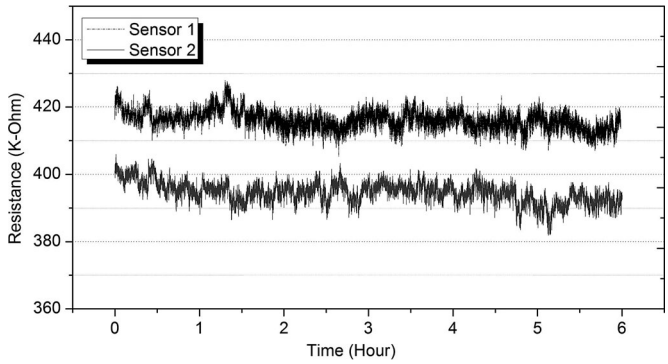

Fig. 5. Stability of f-CNT-based ethanol vapor sensor.

experimental results of f-CNTs for two cycles exhibited a linear *I–V* relationship at first, and self-heating effect starts at around several tens of μA. Then, in the nonlinear region, the resistance dropped as temperature is raised. During the alcohol vapor sensing experiments reported in this paper, the operating currents were well controlled under 10 μA, i.e., within the linear region of f-CNTs. Note that the figure also includes the *I–V* characteristics of nonfunctionalized CNTs (i.e., bare MWNTs) and electronic-grade CNTs (EG-CNTs)-based sensors, which showed a similar *I–V* characteristics trend as f-CNTs, but they were less susceptible to temperature change compared with f-CNTs.

The power consumption (i.e., $P = IV = I^2R$) of the f-CNT-based ethanol sensors is typically around several μW. This ultralow power consumption enables the sensor to pick up the physical parameters with minimal thermal disturbance, which is an indispensable property for sensing true measurands in microscale and nanoscale worlds.

B. Thermal Sensitivity

Temperature coefficient of resistance (TCR) of the f-CNTs was tested to determine the temperature-dependency of their resistance. Classically, the thermal sensitivity of a resistor can be calculated as follows:

$$R = R_{\text{ref}}[1 + \alpha(T - T_{\text{ref}})] \quad (1)$$

where α represents the temperature coefficient of the f-CNT-based sensors, R and R_{ref} represent the resistance at a certain temperature T and reference temperature T_{ref}, respectively.

During the TCR test, an f-CNT-based sensor is exposed to a temperature range of 20 °C to 80 °C at 5 °C increments. During this period, humidity is controlled to be constant at 20% RH. The resistance change of the sensors from our experiments is recorded and shown in Fig. 4, which indicates a negative TCR of approximately –0.206%. This is in accordance with the trend of resistance dropping under relatively higher current in the *I–V* characterization of the sensor. In addition, the TCR of several other types of CNTs are also plotted in Fig. 4 for comparison, which include bare MWNTs, OH-MWNTs (i.e., functionalized MWNTs with OH- groups) and EG-CNTs. For each CNT sensor, at least two cycles of data were collected to prove its repeatability.

C. Stability

Long-term stability is an essential factor to characterize a sensor's performance. In order to evaluate the reliability of f-CNT-based sensors, a 6-h stability test was carried out and the results are shown in Fig. 5. The experiment was conducted in the open environment under room temperature, where the fluctuation of ambient condition was unknown (i.e., there could have been fluctuations in temperature and humidity in the environment). However, the sensor resistance stayed fairly constant during the whole process. The maximum resistance change was 4.99% within 6 h utilizing the activating current of 10 μA.

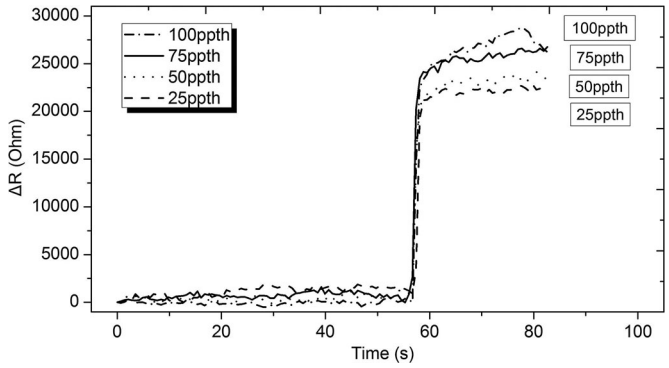

Fig. 6. Typical response of f-CNT-based ethanol vapor sensor.

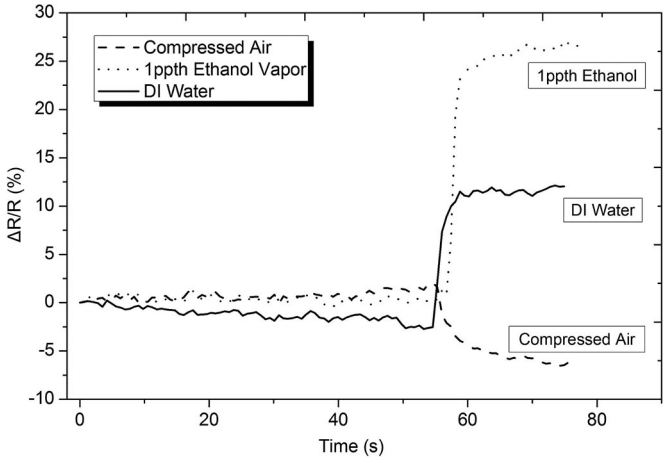

Fig. 7. Selectivity of f-CNT-based ethanol vapor sensor.

IV. F-CNT Sensors for Ethanol Vapor Detection

A. Typical Response

Upon exposure to the ethanol vapor, a sharp increase of the f-CNT sensor resistance was observed. Fig. 6 shows the response of a typical ethanol sensor toward different ethanol concentrations, in which all four curves demonstrated a fast response time. We also found that this change of resistance is reversible. That is, after each measurement, the ethanol solution was withdrawn and compressed air was blown onto the ethanol sensor surface for several seconds, during which resistance dropped instantly. Despite the small amplitude resistance fluctuations, the decreasing resistance usually stopped at almost the same level as its original value. However, in order to make sure that the sensor has been reset to its initial condition, a high current, i.e., 100–200 μA, was added to anneal the sensor for the purpose of burning out all the ethanol molecules attached to the f-CNTs.

B. Selectivity

In order to evaluate the selectivity of the sensor, the responses of a typical ethanol sensor toward dionized (DI) water, ethanol vapor and compressed air were investigated. For the purpose of comparison, the compressed air was kept at 102 kPa, which was the same pressure as used to generate the ethanol vapor in our experiments. Also, the volume of DI water and ethanol solution was both 200 mL. The results of sensor performance toward three media are shown in Fig. 7, where two trends are observed: for DI water and 1 ppth ethanol vapor, the resistance increased, while toward compressed air flow, on the contrary, the resistance dropped. We also found that sensor showed larger response toward the 1 ppth ethanol vapor than DI water. In summary, the ethanol sensor demonstrated good selectivity in differentiating these three media. We note here that air was blown on the sensor surface to increase the conductivity of the CNTs (i.e., resetting the sensors to their initial resistance) after each detection experiment.

C. Mechanism of Ethanol Sensor

The proposed mechanism of f-CNT-based ethanol vapor sensor is that COOH group attached on the CNTs would interact with the OH group of ethanol molecules in the ambient environment through hydrogen bonds, which results in the resistance change of the ethanol vapor sensor. The main chemical reaction is given as follows:

$$-\mathrm{COOH} + \mathrm{OH}^- \rightarrow -\mathrm{COO}^- + \mathrm{H_2O}.$$

This whole process is reversible if we anneal the sensor by blowing compressed air onto the sensor and use relatively high current to heat up the sensor to eliminate the residual molecules.

V. CP Configuration

A. CP Circuit for Ethanol Detection

As we presented previously, during the ethanol vapor detection under CC configuration, the sensor respond to the ethanol vapor by a rising of resistance. However, this response would also result in the increase of power dissipation, most of which are in the form of heat. It is known that self-heating of a sensor will introduce many problems such as larger noise level. The situation is even worse for f-CNT-based ethanol sensors, since the heat generated would possibly burn out the ethanol molecules that are already attached to the sensor surface, which in turn leads to inaccurate measurements. Hence, in order to address the problem and keep the power dissipated on CNT sensor constant, a circuit for CP operation was built (see the inset of Fig. 8) and utilized to achieve better sensor performance.

In this design, a voltage controlled current source (VCCS) was implemented. The system was controlled by the MSP430 uP from TI. During measurement period, the gate voltage of M2 remains high and thus there is no current in this path. When the voltage output at DAC12 increases, the output voltage of the op-amp (V_-) also increases. The system will eventually reach a stable point when current through M2 stops increasing. The relationship between I_{cnt} and V_{dac} is represented in

$$I_{\mathrm{cnt}} = K \times V_{\mathrm{dac}} + C. \tag{2}$$

The TI MSP430FG430 is a 16-bit high-end microcontroller for digital multimeter of DAC and 16 channels ADC all in 12 bits resolution, for analog design. An evaluation board from Soft-Baugh (DG 439 V) powered by a 3 V battery was also interfaced

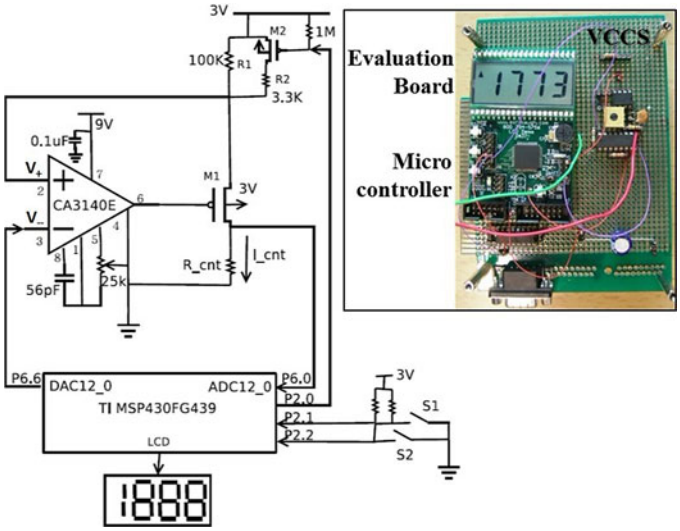

Fig. 8. Circuit diagram: VCCS and MSP430 microcontroller (*inset*: photo of the CP circuit).

to the VCCS circuit in this design. To reduce power consumption, the uP will measure the CNTs sensor resistance and adjust the DAC output four times per second. For rest of the time, the uP will be in low power mode 3 (LPM3) which consumes less than 3 μW according to the TI document. The program flow of the MSP430 application is shown in Fig. 8.

This circuit setup has been used to measure the resistance of CNT sensors under room temperature. During the measurement, data are digitally displayed on an LCD, and resistance change curve are shown on the computer simultaneously by compatible software. In addition, the CP circuit enables the sensor to perform under different power levels, ranging from 0.05 μw to around 2 μw, which is convenient to investigate the relationship between the sensor performance and operating power. We also note that although self-heating can possibly affect the accuracy of measurement, it can be utilized, on the other hand, to clean up the residual ethanol molecules attached on the CNTs. Therefore, the CP circuit also offers the function to anneal the sensor after each cycle of measurement. To sum up, the main functions of the CP circuit include CP operation, data collection, operating power control, and sensor annealing.

Comparison experiments between CC and CP mode were conducted. In the experimental setup of CP configuration, CP circuit was employed to replace the source meter in the CC mode. Other than that, all the experimental variables remained the same for consistency.

B. Sensor Response Versus Power

In Fig. 9, sensor responses versus different power units under four ethanol concentrations were investigated. The ethanol vapor concentrations used were 100, 75, 50, and 25 ppth, respectively. In Fig. 9, the solid lines and dashed lines represent the CP and CC configurations, respectively. The trends in Fig. 9(a)–(d) proved a decrease of response along with the increase of operating power, which implied that the f-CNT-based ethanol sensor tended to perform better under lower operating power. In addi-

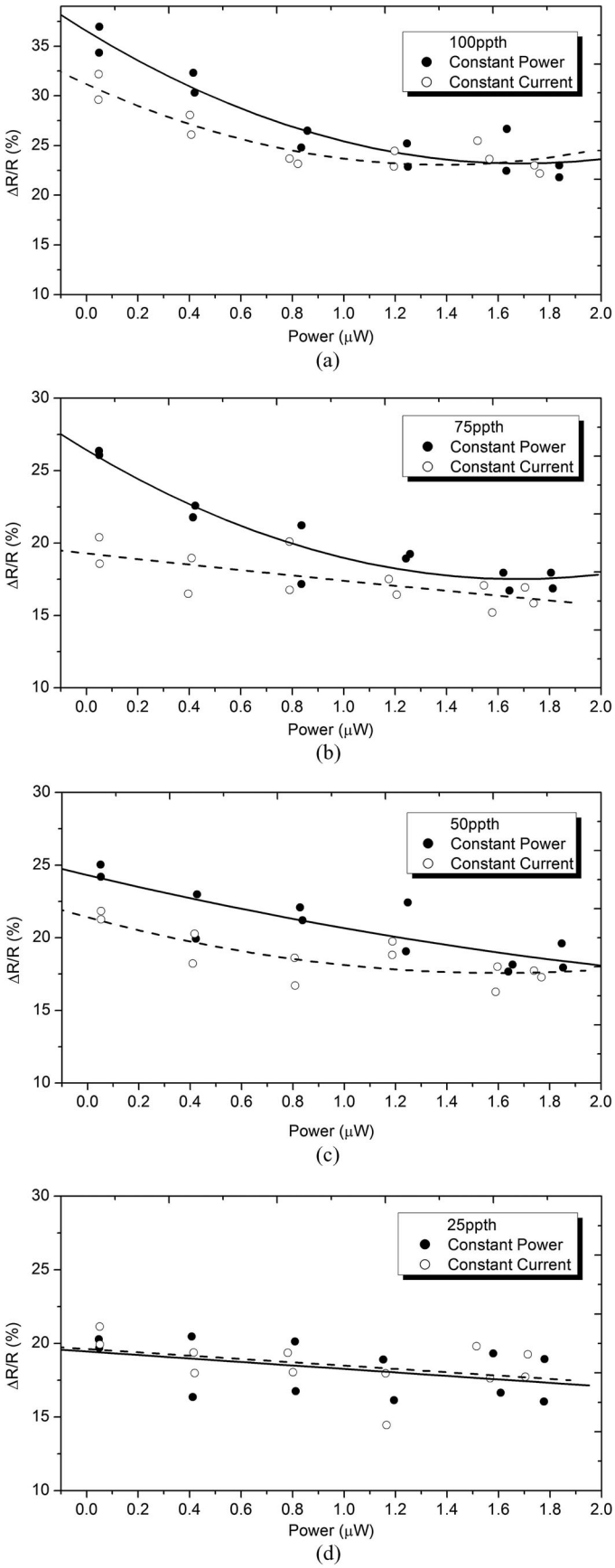

Fig. 9. Response versus operating power. Ethanol concentrations: (a) 100 ppth; (b) 75 ppth; (c) 50 ppth; (d) 25 ppth.

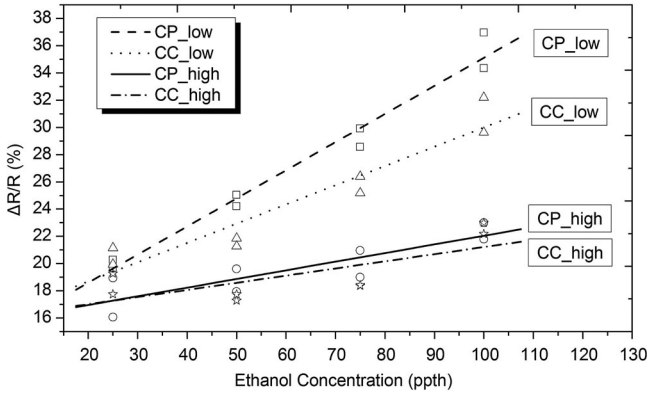

Fig. 10. Response comparison under different ethanol concentrations.

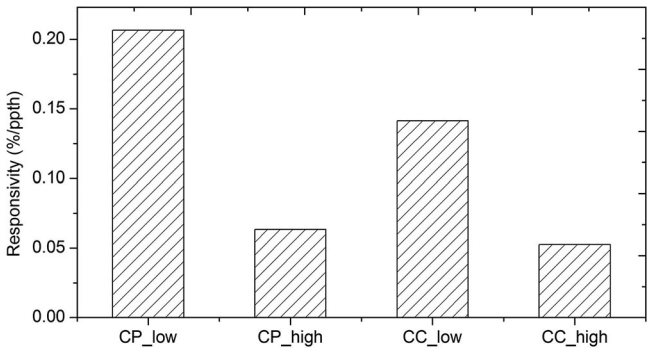

Fig. 11. Responsivity under different conditions.

tion, it is also clearly illustrated that the ethanol sensor exhibited larger response under CP configuration rather than CC mode. However, when the concentration of ethanol vapor was relatively small, e.g., 25 ppth, two response curves almost overlapped, i.e., both configurations exhibit similar response. To sum up, compared to CC configuration, the advantage of CP mode is more obvious under two conditions: lower operating power or higher ethanol vapor concentration.

C. Responsivity

Fig. 10 shows the comparison of four groups of measurements specifying different conditions: CP_low, CC_low, CP_high, and CC_high, where CP and CC stand for the constant-power and constant-current configurations, respectively, while *low* and *high* refer to the operating power of $\sim$0.05 and $\sim$1.8 μW, respectively. For each specified condition, sensor responses under different ethanol vapor concentrations are illustrated in the figure. The slope of fitting curves implies the sensor responsivity, which is definedas follows:

$$\text{Responsivity} = \frac{\text{Response of the sensor}}{\text{Alcohol vapor concentration}}. \tag{3}$$

Also, the responsivities of these four groups are compared in Fig. 11, following the sequence:

$$\text{CP\_low} > \text{CC\_low} > \text{CP\_high} > \text{CC\_high}.$$

The largest responsivity was found in CP_low with the value of 0.2065%/ppth, followed by CC_low as 0.1414%/ppth. On the other hand, CP_high and CC_high exhibited similar responsivities and both much smaller than CP_low. In accordance with the conclusion we drew in the previous section, both CP_low and CC_low proved better responsivity, with the previous one achieved the highest value.

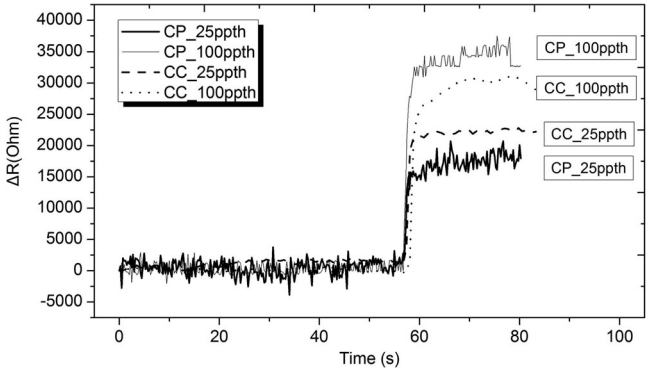

Fig. 12. Noise comparison toward different ethanol concentrations.

D. Noise

All sensors produce some output noise in addition to the output signal [31]. Despite the large resistance change rate, noises during measurements could disturb the true signal severely and jeopardize the accuracy of the sensor. The resistance records of these two different configurations before and after exposure to ethanol vapor are compared in Fig. 12, where the ethanol concentrations were 25 and 100 ppth, respectively. For each cycle of the experiment, the sensor resistance was first monitored for around 57 s as reference. And then, the sensor was successively exposed to ethanol vapor for around 20 s. From the figure, it is clear that CP circuit proved much larger resistance fluctuation toward different ethanol concentrations, both before and after the exposure. The possible explanation is that CP circuit introduced larger noise level than CC mode, especially under lower operating power. It is reasonable because in the CC configuration, the commercial source meter utilized provided better noise reduction system than the CP circuit we built.

E. Sensitivity

Due to the existence of noise, the factor of responsivity alone is not enough to judge the sensor performance. In this case, we evaluated the sensitivity of the ethanol sensor, which is definedas follows:

$$\text{Sensitivity} = \frac{\text{Noise}}{\text{Responsivity}}. \tag{4}$$

According to this definition, the sensitivity of the sensor reflects the smallest detectable ethanol vapor level, i.e., the smaller the calculated value, the higher the sensitivity. Fig. 13 shows the sensitivities of CNT sensor under four conditions; the results are listed as follows:

$$\text{CC\_low} > \text{CP\_low} > \text{CC\_high} > \text{CP\_high}.$$

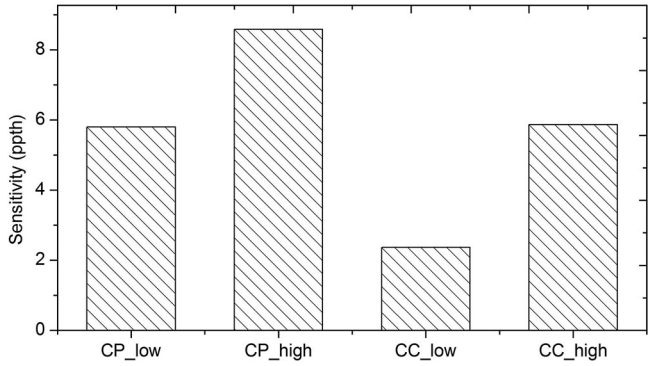

Fig. 13. Sensitivity under different conditions.

Among the four specified conditions, CC_low exhibits the highest sensitivity as 2.366 ppth, followed by the similar sensitivity of CP_low and CC_high. Compared with the responsivities in Fig. 13, we found that although CP_low proved best responsivity. Its sensitivity, however, is not as good as CC_low. However, the sensitivity could be potentially improved if we have better control of the noise level, i.e., better noise reducing component in the CP circuit.

F. Response Time

The time constant, which is the smaller the better, represents the dynamic response of a sensor. During the experiments, the time constants of both CC and CP configurations under different ethanol concentrations have been extracted and compared. Typically, as shown in Fig. 14, sensors under CC mode exhibited larger time constant, i.e., more response time was needed under CC configuration. Also, in Fig. 15, we present the time constant versus ethanol concentration under four different conditions: CP_low, CC_low, CP_high, and CC_high (same representations as in Fig. 10). The results showed that for both operating power, the sensor under CP mode proved its advantage of faster response.

VI. Sensor Response Toward Low Concentrations

Sensors that could detect low concentration ethanol are especially desirable for commercial applications (e.g., drank-driving tests by police forces worldwide). For CNT-based ethanol sensors, the responsivity of the sensor might vary from one sample to another to some extent. Several samples were found to be extremely sensitive and showed large responsivity toward even lower concentration, i.e., below 25 ppth. Fig. 16 shows the result of using an f-CNT-based sensor to detect ethanol vapor between 1 and 10 ppth. The two-probe room temperature resistance of the sensor was around 300 kΩ. During the experiments, we excited the sensor with a current of 0.05 μA, and the approximate power consumption was 8 nW. Experimental data were recorded by a commercial CC source meter. After annealing for 5 min, the sensor was exposed to ethanol vapor for 20 s for each cycle of measurement, and then the sensor response was calculated. For each ethanol concentration (i.e., 1, 5, and 10 ppth), two consecutive tests were carried out to ensure the repeatabil-

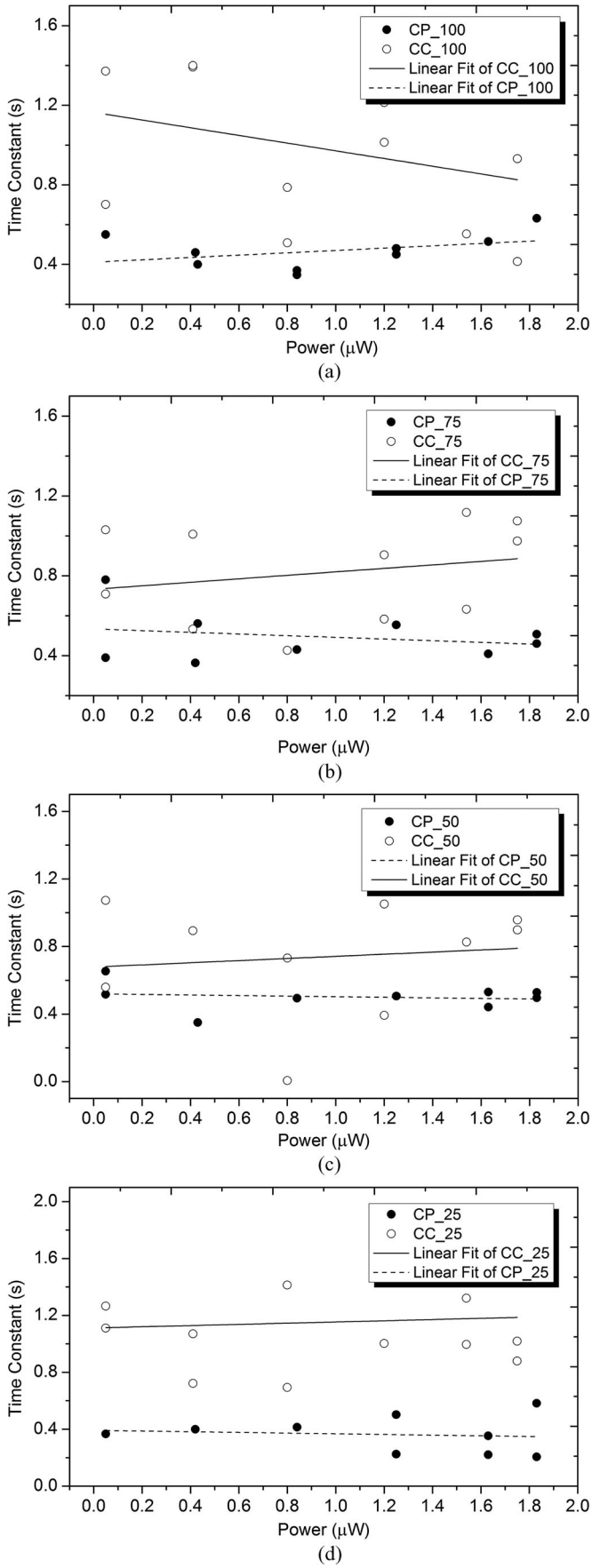

Fig. 14. Time constants versus operating power. Ethanol concentrations: (a) 100 ppth; (b) 75 ppth; (c) 50 ppth; (d) 25 ppth.

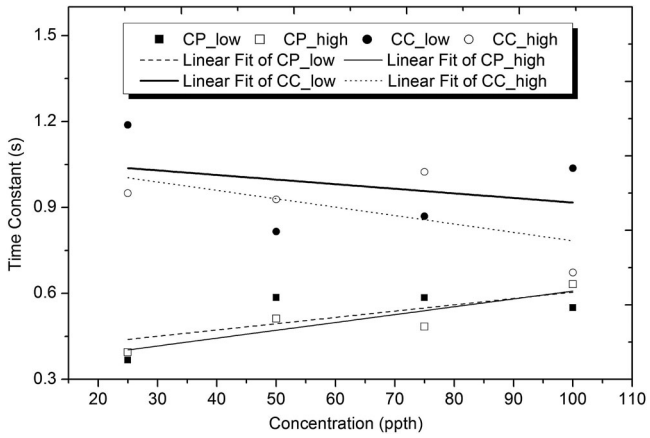

Fig. 15. Time constant comparison under different ethanol concentrations.

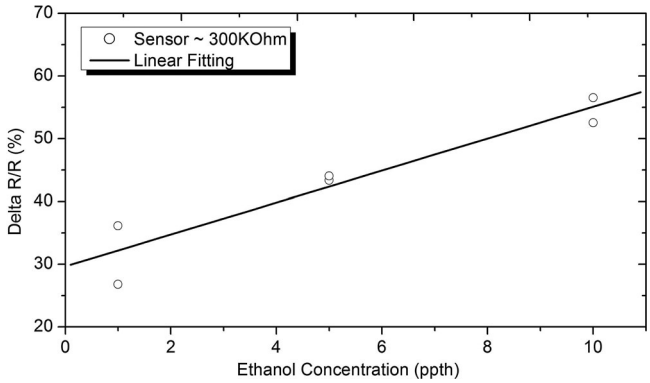

Fig. 16. Response toward low ethanol vapor concentrations.

ity of the sensor and the values of these two measurements are shown in Fig. 16. As illustrated, fitting curve matches the experimental results pretty well and demonstrates good linearity of the sensor. Hence, the capability of f-CNT sensors to detect low ethanol concentration has been validated, which makes them very promising for future commercial applications.

VII. Conclusion

This paper reports our work in comparing CC and CP-based activation of CNT sensors. As an application example, MWCNTs were functionalized with COOH groups to serve as alcohol vapor sensors. The sensors were activated with both CC and CP modes, and their output response are reported and compared in detail in this paper. The functionalized MWCNT (f-CNT) sensors exhibit negative TCR and showed reproducible increase of resistance upon exposure to increasing ethanol vapor concentrations. Experimental results indicate that sensors achieved larger responsivity and faster response time using the CP configuration when compared with the conventional CC mode. Experimental results also show that although f-CNT sensors performed better under lower operating power (for both CC and CP modes), extra noise was also introduced into the system and compromise the sensitivity of the sensor, especially when operating power was lower. Hence, we conclude that, compared to CC activation, CP activation can be used for CNT-based sensors to reduce transient response time, increase responsivity, and reduce power consumption. The sensitivity of the sensors can also be improved if the inherent noise of a CP circuit system can be reduced.

Acknowledgment

The authors would like to thank M. L. Y. Sin and G. C. T. Chow for their extensive discussion of this project. They would also like to thank Brittle K. H. Tsoi for building the CP circuit used in this project. W. J. Li would also like to thank The Chinese University of Hong Kong for its continual support of his graduate students in the Centre for Micro and Nano Systems, where many of the results presented in this paper were collected.

References

[1] S. Reich, C. Thomsen, and J. Maultzsch, *Carbon Nanotubes, Basic Concepts and Physical Properties*. Berlin: Wiley, 2004, pp. 3–30.

[2] R. H. Baughman, A. A. Zakhidov, and W. A. de Heer, "Carbon Nanotubes—the route toward applications," *Science*, vol. 297, pp. 787–792, 2002.

[3] S. Peng, J. O'Keeffe, C. Wei, and K. Cho, "Carbon nanotube chemical and mechanical sensors," in *Proc. 3rd Int. Workshop on Structual Health Monitoring*, 2004, pp. 1–8.

[4] J. Kong, N. R. Franklin, C. Zhou, M. G. Chapline, S. Peng, K. Cho, and H. Dai, "Nanotube molecular wires as chemical sensors," *Science*, vol. 287, pp. 622–625, 2000.

[5] M. H. Tsai, H. M. Lin, W. L. Tsai, and Y. Hwu, "Examined the gas absorption properties of single wall carbon nanotube bundles by X-ray absorption techniques," *Rev. Adv. Mater. Sci*., vol. 5, pp. 302–305, 2003.

[6] W. Shi and J. Karl Johnson, "Gas adsorption on heterogeneous single-walled carbon nanotube bundles," *Phy. Rev. Lett*., vol. 91, pp. 0155041–0155044, 2003.

[7] A. Fujiwara, K. Ishii, H. Suematsu, H. Kataura, Y. Maniwa, and S. Suzuki *et al*., "Gas adsorption in the inside and outside of single-walled carbon nanotubes," *Chem. Phy. Lett*., vol. 336, pp. 205–211, 2001.

[8] O. K. Varghese, P. D. Kichambre, D. Gong, K. G. Ong, E. C. Dickey, and C. A. Grimes, "Gas sensing characteristics of multi-wall carbon nanotubes," *Sens. Actuators B, Chem*., vol. 81, pp. 32–41, 2001.

[9] K. Ghee Ong, K. Zeng, and C. A. Grimes, "A wireless, passive carbon nanotube-based gas sensor," *IEEE Sens. J*., vol. 2, no. 2, pp. 82–88, Apr. 2002.

[10] K. H. An, S. Y. Jeong, H. R. Hwang, and Y. H. Lee, "Enhanced sensitivity of a gas sensor incorporating single-walled carbon nanotube-polypyrrole nanocomposites," *Adv. Mater*., vol. 16, pp. 1005–1009, 2004.

[11] J. Suehiro, G. Zhou, and M. Hara, "Fabrication of a carbon-nanotube-based gas sensor using dielectrophoresis and its application for ammonia detection by impedance spectroscopy," *J. Phys. D: Appl. Phys*., vol. 36, pp. L109–L114, 2003.

[12] Y. W. Chang, J. S. Oh, S. H. Yoo, H. H. Choi, and K. H. Yoo, "Electrically refreshable carbon-nanotube-based gas sensors," *Nanotechnology*, vol. 18, pp. 1–4, 2007.

[13] D. Ding, Z. Chen, S. Rajaputra, and V. Singh, "Hydrogen sensors based on aligned carbon nanotubes in an anodic aluminum oxide template with palladium as a top electrode," *Sens. Actuators. B, Chem*., vol. 124, pp. 12–17, 2007.

[14] J. K. Abraham, B. Philip, A. Witchurch, V. K. Varadan, and C. C. Reddy, "A compact wireless gas sensor using a carbon nanotube/PMMA thin film chemiresistor," *Smart Mater. Struct*., vol. 13, pp. 1045–1049, 2004.

[15] J. Maklin, T. Mustonen, K. Kordas, S. Saukko, G. Toth, and J. Vahakangas, "Nitric oxide gas sensors with functionalized carbon nanotubes," *Phys. Stat. Sol*., vol. 244, pp. 4298–4302, 2007.

[16] L. Y. Sin, C. T. Chow, M. K. Wong, Wen J. Li, H. W. Leong, and K. W. Wong, "Ultra-low-power alcohol vapor sensors using chemically functionalized multi-walled carbon nanotubes," *IEEE Trans. Nanotechnol*., vol. 6, no. 5, pp. 571–577, 2007.

[17] K. M. Fung, Q. H. Zhang, Z. Dong, and Wen J. Li. "Fabrication of CNT-based MEMS piezoresistive pressure sensors using DEP nanoassembly," in *Proc. IEEE 5th Conf. Nanotechnol*., 2005, vol. 1, pp. 199–202.

[18] Y. L. Qu, W. Y. Chow, M. X. Ouyang, C. H. Tung, WenJ. Li, and X. L. Han, "Ultra-low-powered aqueous shear stress sensors based on bulk EG-CNTs integrated in microfluidic systems," *IEEE Trans. Nanotechnol.*, vol. 7, no. 5, pp. 565–572, Sep. 2008.
[19] K. Uchida, S. Okada, K. Shiraishi, and A. Oshiyma, "Quantum effects in a double-walled carbon nanotube capacitor," *Phys. Rev. B*, vol. 76, p. 155436-1-9, 2007.
[20] M. Budnik, A. Raychowdhury, A. Bansal, and K. Roy, "A high density, carbon nanotube capacitor for decoupling applications," in *Proc. IEEE 43rd Annu. Conf. Design Autom.*, 2006, pp. 935–938.
[21] G. Chen, S. Bandow, E. R. Margine, C. Nisoli, A. N. Kolmogorov, V. H. Crespi *et al.*, "Chemically doped double-walled carbon nanotubes: cylindrical molecular capacitors," *Phys. Rev. Lett.*, vol. 90, p. 257403-1-4, 2003.
[22] E. S. Snow, F. K. Perkins, E. J. Houser, S. C. Badescu, and T. L. Reinecke, "Chemical detection with a single-walled carbon nanotube capacitor," *Science*, vol. 307, pp. 1942–1945, 2005.
[23] A. Javey, J. Guo, Q. Wang, M. Lundstrom, and H. Dai, "Ballistic carbon nanotube field-effect transistors," *Nature*, vol. 424, pp. 654–657, 2003.
[24] J. Li, Y. Lu, Q. Ye, M. Cinke, J. Han, and M. Meyyappan, "Carbon nanotube sensors for gas and organic vapor detection," *Nano Lett.*, vol. 3, pp. 929–933, 2003.
[25] G. L. Anderson and D. M. Hadden, *The gas Monitoring Handbook*. New York: Avocet Press, Inc., pp. 74–76, 1999.
[26] S. W. Chan and C. H. Chan, "A resistance variation tolerant constant power heating circuit for integrated sensor applications," *IEEE J. Sol.-Stat. Circuits*, vol. 34, no. 4, pp. 432–439, Apr. 1999.
[27] K. A. Makinwa and J. H. Huijsing, "Constant power operation of a two-dimensional flow sensor using thermal sigma-delta modulation techniques," in *Proc. IEEE Instrum. Meas. Tech. Conf.*, pp. 1577–1580, 2001.
[28] (2009). [Online]. Available: http://www.e2v.com/e2v/assets/File/sensors_datasheets/metal_oxide/MICS-5525.pdf
[29] L. Y. Sin, C. T. Chow, K. M. Fung, Wen J. Li, H. W. Leong, K. W. Wong, and T. Lee, "Ultra-low-power alcohol vapor sensors based on multi-walled carbon nanotube," in *Proc. IEEE Int. Conf. Nano/Micro Eng. Syst.*, Jan. 18–21, 2006, pp. 1198–1202.
[30] T. S. Wong and Wen J. Li, "Bundled carbon nanotubes as electronic circuit and sensing elements," in *Proc. IEEE Int. Conf. Robot. Autom.*, 2003, vol. 3, pp. 3648–3653.
[31] J. S. Wilson, *Sensor Technology Handbook*. Amsterdam, Boston: Elsevier, pp. 2–3.

Mengxing Ouyang received the B.Eng. degree majoring in biomedical engineering from the Huazhong University of Science & Technology, Wuhan, China, and the M.Phil. degree in the application of micro/nano sensors based on carbon nanotubes from the Centre for Micro and Nano Systems, The Chinese University of Hong Kong, Hong Kong, in 2009. She is currently working toward the Ph.D. degree in the Department of Mechanical and Automation Engineering in the same university. Her current research interest includes nano-bio-sensors and using DEP force for biomanipulation.

Wen J. Li (F'11) received the B.S.A.E. and M.S.A.E. degrees from the University of Southern California, Los Angeles, in 1987 and 1989, respectively, and the Ph.D. degree in aerospace engineering from the University of California, Los Angeles, in 1997.

Since November 2011, he has been with the Department of Mechanical and Biomedical Engineering of the City University of Hong Kong (CityU), Kowloon, Hong Kong. From September 1997 to October 2011, he was with the Department of Mechanical and Automation Engineering, The Chinese University of Hong Kong. His industrial experience includes The Aerospace Corporation (El Segundo, CA), NASA Jet Propulsion Laboratory (Pasadena, CA), and Silicon Microstructures, Inc. (Fremont, CA). His research interests include nanoscale fabrication, sensing, and manipulation.

Dr. Li currently serves as the Editor-in-Chief of the IEEE Nanotechnology Magazine.

Philip H. W. Leong received the B.Sc., B.E. and Ph.D. degrees from the University of Sydney, Sydney, Australia.

In 1993, he was a consultant to ST Microelectronics, Milan, Italy working on advanced flash memory-based integrated circuit design. From 1997–2009 he was with The Chinese University of Hong Kong, Shatin, Hong Kong. He is currently an Associate Professor in the School of Electrical and Information Engineering at the University of Sydney. He is also a Visiting Professor at Imperial College, London, U.K. and the Chief Technology Consultant at Cluster Technology. He was the Cofounder and Program Cochair of the International Conference on Field Programmable Technology (FPT) and the International Conference on Field Programmable Logic and Applications (FPL), and is an Associate Editor of the ACM Transactions on Reconfigurable Technology and Systems. He is the author of more than 100 technical papers and 4 patents.

Dr. Leong was the recipient of the 2005 FPT Conference Best Paper as well as the 2007 and 2008 FPL Conference Stamatis Vassiliadis Outstanding Paper awards.

Ka Wai Wong received the B. Sc., M. Phil. and Ph.D. degrees in chemistry from The Chinese University of Hong Kong (CUHK), Shatin, Hong Kong, in 1992, 1995, and 1999, respectively.

After graduation, he joined the Advanced Surface and Materials Analysis Centre as Programme Executive and then joined the Department of Physics, CUHK as Postdoctoral Fellow with major research focus on organic/polymeric optoelectronics. From 2003–2005, he was with Hong Kong DNA Chips Limited as a Project Manager leading an R&D team on developing novel silicon-based DNA chips for molecular diagnostics. He is currently with the Nano and Advanced Materials Institute Limited, Kowloon, Hong Kong. He is also a Visiting Research Scientist in Chengdu Green Energy and Green Manufacturing Technology R&D Center, Sichuan, China, a Guest Professor in the State Key Laboratory of Metal Matrix Composites, Shanghai Jiao Tong University, Shanghai, China, and an Adjunct Professor in the Institute of Surface Micro and Nano Materials, Xuchang University, Xuchang, China. His major research interests include nanotechnology, sensing technology, surface science, and materials engineering.